JOINT DESIGN OF MULTI-TAP FILTERS AND POWER CONTROL FOR FBMC/OQAM BASED TWO-WAY DECODE-AND-FORWARD RELAYING SYSTEMS IN HIGHLY FREQUENCY SELECTIVE CHANNELS

Jianshu Zhang, Ahmad Nimr, and Martin Haardt

Communications Research Laboratory, Ilmenau University of Technology
P. O. Box 10 05 65, 98684 Ilmenau, Germany

ABSTRACT

In this paper we study the achievable rate region of an FBMC based two-way decode-and-forward relaying system. Unlike a CP-OFDM system, the FBMC based systems experience inter-carrier interference and inter-symbol interference especially in a highly frequency selective channel. To calculate the resulting rate region, we have to solve a joint optimization of the per-subcarrier multi-tap filters at the relay as well as at the users, which is non-convex. Therefore, we resort to a two-step approach. First, we design closed-form solutions for the per-subcarrier pre-equalizers and equalizers at all nodes. Then we derive an optimal power allocation scheme to maximize the achievable rate. Simulation results show that the achievable sum rate increases as the number of taps used for pre-equalization and equalization at the subcarriers increases.

Index Terms— FBMC, two-way relaying, decode and forward, multi-tap filters, power allocation, convex optimization.

I. INTRODUCTION

Filter-bank multi-carrier (FBMC)/Offset-QAM (OQAM) is an attractive multi-carrier modulation technique since it does not transmit an additional cyclic prefix (CP) and its subcarrier signals are shaped with waveforms that have significantly less spectral leakage than CP-OFDM [1], [2]. In general, due to the use of OQAM modulation schemes, orthogonality between subcarriers can be realized in multi-path fading scenarios. Thus, single-tap equalizer techniques for OFDM system can be directly implemented. However, when the channel is highly frequency selective, the inter-symbol interference (ISI) and inter-carrier interference (ICI) is inevitable unless the modulated signal is filtered by multi-tap pre-equalizers and/or equalizers [3]. Multi-tap filter designs have been considered for point-to-point (P2P) channels [4]. Previous works on FBMC based two-way relaying (TWR) systems include [5] and [6]. They study only power allocation and relay scheduling schemes in a cognitive radio context. They do not consider the ISI and ICI and thus are not suitable for highly frequency selective channels.

In this paper we study the design of the multi-tap filters as well as the power control scheme for FBMC/OQAM coded two-way decode-and-forward (DF) relaying systems in a highly frequency selective channel. The goal is to obtain the achievable rate region subject to transmit power constraints at all nodes. To this end, a joint design of the pre-equalizers and equalizers at the relay as well as at the user terminals (UTs) over all subcarriers is required. To avoid an intractable optimization problem, we resort to sub-optimal solutions. That is, we first determine the pre-equalizer and equalizer schemes. The optimization problem is then turned into a power allocation problem, which is still non-convex due to the existence of residual ICI and ISI. We devise an efficient polynomial time convex optimization based algorithm to solve this problem. The developed algorithm can be viewed as an extension of the polynomial time DC (POTDC) solution in [7]. Simulation results show that the achievable rate of the FBMC/OQAM based relaying system increases as the number of filter taps used for pre-equalization and equalization at each subcarrier increases.

II. SYSTEM MODEL

We consider a three-node TWR system, where two UTs (UT1 and UT2) communicate with each other via the help of a DF relay. Every node has a single antenna and operates in a half-duplex mode. A complete transmission takes two time slots. In the first time slot, also known as the multiple access channel (MAC) phase, both UTs transmit to the relay. To combat the strong time dispersion of the channel, a multi-tap pre-equalizer $a_{i,m}[k]$ ($i \in \{1,2\}$ and $m \in \{1, \cdots M\}$) is applied per subcarrier per UT before the OQAM symbols $x_{i,m}[k] = d_{i,m}[k]\theta_{i,m}[k]$ pass through a low-pass filter $f_m[n]$, i.e., the synthesis filter bank (SFB) [4]. The transmitted FBMC/OQAM signal from the i-th UT is thus written as [8]

$$s_i[n] = \sum_{m=0}^{M-1} \sum_{k=-\infty}^{+\infty} \sqrt{P_{i,m}}(x_{i,m}[k] * a_{i,m}[k]) \cdot f_m\left[n - k\frac{M}{2}\right]$$

where $f_m[n] = p[n]e^{j\frac{2\pi m}{M}(n-\frac{(4M-1)}{2})}$ and $p[n]$ is the prototype filter, which is defined in the same way as in [4]. The signal $d_{i,m}[k]$ denotes the real symbol drawn from a PAM constellation with zero mean and unit variance and $\theta_{i,m}[k]$ is used for generating the corresponding OQAM symbol, where $\theta_{i,m}[k] = 1$ if $(m+k)$ is even and $\theta_{i,m}[k] = j$ if $(m+k)$ is odd. Note that due to the rate conversion different sampling indices have been used, where the index n represents the high rate signals while the index k represents the low rate signals. The energy of the prototype filter is normalized such that $\sum_{n=-\infty}^{+\infty} |p[n]|^2 = 1$ [8]. The variable $P_{i,m}$ denotes the transmit power allocated to the m-th subcarrier of the i-th UT. A transmit power constraint at the i-th UT has to be fulfilled such that $\sum_{n=-\infty}^{+\infty} \mathbb{E}\{|s_i[n]|^2\} \leq P_{\mathrm{U}}$, $\forall i$.

Let $h_{i,\mathrm{R}}[n]$ denote the channel impulse responses (CIRs) from the i-th UT to the relay, $\forall i$. The received signal at the relay is

$$r[n] = \sum_{i=1}^{2} h_{i,\mathrm{R}}[n] * s_i[n] + \nu_{\mathrm{R}}[n], \tag{1}$$

where $\nu_{\mathrm{R}}[n]$ denotes zero-mean circularly symmetric complex Gaussian (ZMCSCG) noise. The relay uses a DF relaying strategy. Thus, it decodes and re-encodes the received signal. The decoding process starts by feeding the received signal to the analysis filter bank (AFB) [4]. Following a similar manipulation as in [4], the filtered complex data on the q-th subcarrier at the k-th instant at the relay is then obtained as

$$\tilde{r}_q[k] = \sum_{m=q-1}^{q+1} \sum_{i=1}^{2} \sqrt{P_{i,m}} b_{\mathrm{R},q}[k] * x_{i,m}[k] * a_{i,m}[k] * g_{i,q,m}[k] + b_{\mathrm{R},q}[k] * \tilde{\nu}_{\mathrm{R},q}[k],$$

where $b_{\mathrm{R},q}[k]$ is the per-subcarrier multi-tap equalizer at the relay, $g_{i,q,m}[k] = (f_m[n] * h_{i,\mathrm{R}}[n] * f_q^*[-n])_{\downarrow\frac{M}{2}}$, and $\tilde{\nu}_{\mathrm{R},q}[k] = (\nu_{\mathrm{R}}[n] * f_q^*[-n])_{\downarrow\frac{M}{2}}$, where $(\cdot)_{\downarrow\frac{M}{2}}$ represents the downsampling by a factor $\frac{M}{2}$ and the ZMCSCG noise term $\tilde{\nu}_{\mathrm{R},q}[k]$ has variance σ_{R}^2. To estimate the binary messages of the UTs, it is useful to extract the real part of the received signal, i.e., $\hat{r}_q[k] = \Re\{\theta_q^*[k]\tilde{r}_q[k]\}$, where $\Re\{\cdot\}$ denotes the real part [8]. After the binary information is recovered, a network coding scheme should be applied. Here it is assumed that an optimal network coding scheme is used [9]. Let $x_{\mathrm{R},m}[k] = d_{\mathrm{R},m}[k]\theta_{\mathrm{R},m}[k]$ denote the OQAM symbols, which contain the network coded binary information for both UTs. Again, per-subcarrier multi-tap pre-equalizers $a_{\mathrm{R},m}[k]$ are utilized by the relay to counteract the channel fading effects. In the second time slot, also known as the broadcasting channel (BC) phase, the transmitted FBMC/OQAM signal from the relay is expressed as

$$\bar{r}[n] = \sum_{m=0}^{M-1}\sum_{k=-\infty}^{+\infty}\sqrt{P_{\mathrm{R},m}}(x_{\mathrm{R},m}[k] * a_{\mathrm{R},m}[k])f_m\left[n - k\frac{M}{2}\right].$$

The transmit power constraint at the relay has to be fulfilled such that $\sum_{n=-\infty}^{+\infty}\mathbb{E}\{|\bar{r}[n]|^2\} \le P_{\mathrm{R}}$.

Let us define the CIR from the relay to the j-th UT as $h_{\mathrm{R},j}[n]$, where $j \in \{1,2\}$ and $j \neq i$. At the receiver side of the j-th UT, a similar decoding procedure as at the relay is performed. Moreover, let us define the per-subcarrier multi-tap equalizer at the j-th UT as $b_{j,m}[k]$. Then the received complex-valued signal on the q-th subcarrier at the k-th instant of the j-th UT is derived as

$$\begin{aligned} y_{j,q}[k] = &\sum_{m=q-1}^{q+1}\sqrt{P_{\mathrm{R},m}}b_{j,q}[k] * x_{\mathrm{R},m}[k] * a_{\mathrm{R},m}[k] * \hat{g}_{j,q,m}[k] \\ &+ b_{j,q}[k] * \tilde{\nu}_{j,q}[k], \end{aligned}$$

where $\hat{g}_{j,q,m}[k] = (f_m[n] * h_{\mathrm{R},j}[n] * f_q^*[-n])_{\downarrow\frac{M}{2}}$, $\tilde{\nu}_{\mathrm{R},q}[k] = (\nu_j[n] * f_q^*[-n])_{\downarrow\frac{M}{2}}$, and $\tilde{\nu}_{j,q}[k]$ is the per-subcarrier ZMCSCG noise with variance σ_{U}^2, $\forall q, j$.

Our goal is to design the pre-equalizers ($a_{i,m}[k]$ and $a_{R,m}[k]$) and the equalizers ($b_{\mathrm{R},m}[k]$, $b_{i,m}[k]$) as well as the power allocation schemes ($P_{i,m}$, $P_{\mathrm{R},m}$) at the UTs and at the relay such that the achievable rate of the system is maximized.

III. FIXED DESIGN OF THE EQUALIZERS AND THE PRE-EQUALIZERS

Before we formulate the rate optimization problem, it is worth mentioning that the joint design of multi-tap equalizers and pre-equalizers is difficult and might be intractable. This is because different subcarriers are coupled due to the ICI and ISI, which is well-known for FBMC-based P2P systems [4]. A single tap filter would be much easier to handle but provides only a limited performance improvement in a highly frequency selective channel. Therefore, inspired by [4], we consider pairing the multi-tap equalizers (pre-equalizers) and single tap pre-equalizers (equalizers) in the MAC and the BC phase. This results in a suboptimal solution but it provides a trade-off between the computational complexity and the performance improvement. More specifically, in the MAC phase, both UTs use multi-tap pre-equalizers and the relay uses single tap equalizers, i.e., $b_{\mathrm{R},m}[k] = 1$, $\forall m, k$. In the BC phase, the UTs use multi-tap equalizers while the relay uses again single tap pre-equalizers with $a_{\mathrm{R},m}[k] = 1$, $\forall m, k$. In the rest of this section our goal is to design pre-equalization and equalization strategies when $P_{i,m}$ and $P_{\mathrm{R},m}$ are set to 1, $\forall i, m$. After this, we formulate the desired signal power and the interference power as a function of more general power allocation vectors.

With the above settings, it is possible to express the real-valued received signal $\hat{r}_q[k]$ in a vector-matrix form, i.e.,

$$\begin{aligned} \hat{r}_q[k] = &\sum_{m=q-1}^{q+1}\sum_{i=1}^{2}\sqrt{P_{i,m}}\boldsymbol{a}_{i,m}^{\mathrm{T}}\boldsymbol{G}_{i,q,m}[k]\boldsymbol{d}_{i,m}[k] + \Re\{\tilde{\nu}_{\mathrm{R},q}[k]\} \\ = &\underbrace{\sum_{i=1}^{2}\sqrt{P_{i,q}}\boldsymbol{a}_{i,q}^{\mathrm{T}}\boldsymbol{G}_{i,q,q}[k]e_\ell d_{i,q}[k]}_{\text{desired signal}} \\ &+\underbrace{\sum_{i=1}^{2}\sum_{\bar{\ell}=1,\bar{\ell}\neq\ell}^{1+L_{a_1}+L_{a_2}+L_{g1}+L_{g2}}\sqrt{P_{i,q}}\boldsymbol{a}_{i,q}^{\mathrm{T}}\boldsymbol{G}_{i,q,q}[k]e_{\bar{\ell}}d_{i,q,\bar{\ell}}[k]}_{\text{inter-symbol interference}} \\ &+\underbrace{\sum_{i=1}^{2}\sum_{\bar{m}=q-1,\bar{m}\neq q}^{q+1}\sqrt{P_{i,\bar{m}}}\boldsymbol{a}_{i,\bar{m}}^{\mathrm{T}}\boldsymbol{G}_{i,q,\bar{m}}[k]\boldsymbol{d}_{i,\bar{m}}[k]}_{\text{inter-carrier interference}} + \Re\{\tilde{\nu}_{\mathrm{R},q}[k]\} \end{aligned}$$

where $\boldsymbol{d}_{i,m}[k] = [d_{i,m}[k + L_{a_1} + L_{g1}] \quad \cdots \quad d_{i,m}[k - L_{a_2} - L_{g2}]]^{\mathrm{T}}$, $\boldsymbol{a}_{i,m} = \left[\Re\{\bar{\boldsymbol{a}}_{i,m}\}^{\mathrm{T}} \quad \Im\{\bar{\boldsymbol{a}}_{i,m}\}^{\mathrm{T}}\right]^{\mathrm{T}} \in \mathbb{R}^{2(1+L_{a_1}+L_{a_2})}$, and $\bar{\boldsymbol{a}}_{i,m} = [a_{i,m}[-L_{a_1}] \cdots a_{i,m}[L_{a_2}]]^{\mathrm{T}} \in \mathbb{C}^{1+L_{a_1}+L_{a_2}}$ for $i = 1, 2$. It is assumed that $L_{a_1} = L_{a_2} = L_a$. The matrices $\boldsymbol{G}_{i,q,m}[k] = \left[\Re\{\bar{\boldsymbol{G}}_{i,q,m}\}^{\mathrm{T}} \quad \Im\{\bar{\boldsymbol{G}}_{i,q,m}\}^{\mathrm{T}}\right]^{\mathrm{T}}$ and $\bar{\boldsymbol{G}}_{i,q,m} \in \mathbb{C}^{(1+2L_a)\times(1+2L_a+L_{g1}+L_{g2})}$ denote the convolution matrix of the effective channel $g_{i,q,m}[k]$, which is block Toeplitz. The indices L_{g1} and L_{g2} depend on the excess delay of the channels and the pulse length of the prototype filter [4]. The column selection vector $\boldsymbol{e}_\ell$ is defined as the ℓ-th column of the identity matrix $\boldsymbol{I}_{1+2L_a+L_{g1}+L_{g2}}$, where $\ell = 1 + L_a + L_{g1}$. We propose to design the augmented pre-equalization vectors $\boldsymbol{a}_{i,m}$ such that the signal-to-leakage-plus-noise ratio (SLNR) is maximized. This design is suboptimal but it allows computing each $\boldsymbol{a}_{i,m}$ independently. Thereby, the desired signal power of the the i-th UT on the q-th subcarrier is calculated as $P_{i,q,\mathrm{sig}} = \mathbb{E}\{|\sqrt{P_{i,q}}\boldsymbol{a}_{i,q}^{\mathrm{T}}\boldsymbol{G}_{i,q,q}[k]\boldsymbol{e}_\ell d_{i,q}[k]|^2\} = \boldsymbol{a}_{i,q}^{\mathrm{T}}\boldsymbol{\Omega}_{i,q}\boldsymbol{a}_{i,q}$, where $\boldsymbol{\Omega}_{i,q} = P_{i,q}\boldsymbol{G}_{i,q,q}[k]\boldsymbol{e}_\ell\boldsymbol{e}_\ell^{\mathrm{T}}\boldsymbol{G}_{i,q,q}[k]^{\mathrm{T}}$. The leaked signal power from the q-th subcarrier of i-th UT includes both the ISI and the ICI that it introduces to the two adjacent subcarriers. It is calculated as $P_{i,q,\mathrm{leak}} = \boldsymbol{a}_{i,q}^{\mathrm{T}}\boldsymbol{\Lambda}_{i,q}\boldsymbol{a}_{i,q}$, where $\boldsymbol{\Lambda}_{i,q} = P_{i,q}\boldsymbol{G}_{i,q,q}[k](\boldsymbol{I} - \boldsymbol{e}_\ell\boldsymbol{e}_\ell^{\mathrm{T}})\boldsymbol{G}_{i,q,q}[k]^{\mathrm{T}} + \sum_{\bar{m}=q-1,\bar{m}\neq q}^{q+1}P_{i,q}\boldsymbol{G}_{i,\bar{m},q}[k]\boldsymbol{G}_{i,\bar{m},q}[k]^{\mathrm{T}}$. Let $\|\boldsymbol{a}_{i,q}\| = 1$ and let us define the SLNR of the i-th UT on the q-th subcarrier as

$$\mathrm{SLNR}_{i,q} = \frac{\boldsymbol{a}_{i,q}^{\mathrm{T}}\boldsymbol{\Omega}_{i,q}\boldsymbol{a}_{i,q}}{\boldsymbol{a}_{i,q}^{\mathrm{T}}\boldsymbol{\Lambda}_{i,q}\boldsymbol{a}_{i,q} + \sigma_{\mathrm{R}}^2/2} = \frac{\boldsymbol{a}_{i,q}^{\mathrm{T}}\boldsymbol{\Omega}_{i,q}\boldsymbol{a}_{i,q}}{\boldsymbol{a}_{i,q}^{\mathrm{T}}(\boldsymbol{\Lambda}_{i,q} + \boldsymbol{I}\sigma_{\mathrm{R}}^2/2)\boldsymbol{a}_{i,q}}. \tag{2}$$

Then the maximization problem $\max_{\boldsymbol{a}_{i,q}}\mathrm{SLNR}_{i,q}$ is a generalized Rayleigh quotient problem. The optimal solution is $\mathcal{P}_{\max}\{(\boldsymbol{\Lambda}_{i,q} + \boldsymbol{I}\sigma_{\mathrm{R}}^2/2)^{-1}\boldsymbol{\Omega}_{i,q}\}$, where $\mathcal{P}_{\max}\{\cdot\}$ computes the dominant eigenvector of a square matrix.

Similarly, the received real-valued signal $\hat{y}_{j,q} = \Re\{\theta_{j,q}^*[k]y_{j,q}[k]\}$ on the q-th subcarrier of the j-th UT is

$$\hat{y}_{j,q}[k] = \sum_{m=q-1}^{q+1}\sqrt{P_{\mathrm{R},m}}\boldsymbol{b}_{j,q}^{\mathrm{T}}\tilde{\boldsymbol{G}}_{j,q,m}[k]\boldsymbol{d}_{\mathrm{R},m}[k] + \boldsymbol{b}_{j,q}^{\mathrm{T}}\bar{\boldsymbol{\nu}}_{j,q}[k] \tag{3}$$

where $\boldsymbol{b}_{j,q}$, $\tilde{\boldsymbol{G}}_{j,q,m}[k]$, and $\boldsymbol{d}_{\mathrm{R},m}[k]$ have the same form as $\boldsymbol{a}_{j,m}$, $\boldsymbol{G}_{i,q,m}[k]$, and $\boldsymbol{d}_{i,m}[k]$ by changing L_{a_1} to L_{b_1}, L_{a_2} to L_{b_2}, and $g_{i,q,m}[k]$ to $\hat{g}_{j,q,m}[k]$. The design strategy is chosen such that the equalizers at different UTs and different subcarriers are devised independently. To this end, we choose the maximization of the SINR as the design criterion, i.e., we maximize the achievable

SINR on each subcarrier of each UT [4]. It should not be difficult to foresee that a generalized Rayleigh quotient problem is formulated and an optimal $\boldsymbol{b}_{j,q}$ is obtained in a closed-form. Again, $\boldsymbol{b}_{j,q}$ is normalized to have unit norm. The details are omitted here due to the space limitation.

As long as the multi-tap filters at the UTs are fixed, we can calculate the signal power as well as the interference power on each subcarrier of each UT as a function of the power allocation vectors $\boldsymbol{p}_i = [P_{i,1} \quad \cdots \quad P_{i,M}]$ and $\boldsymbol{p}_{\mathrm{R}} = [P_{\mathrm{R},1} \quad \cdots \quad P_{\mathrm{R},M}]$. This is important for the design of optimal power control schemes in the next section. For notational simplicity, we will drop the time index k from now on. Then the received signal power at the m-th subcarrier of the relay and from the i-th UT is computed as $P_{i\mathrm{R},m,\mathrm{sig}} = \bar{\boldsymbol{h}}_{i,\mathrm{R},m}^{\mathrm{T}} \boldsymbol{p}_i$. The vector $\bar{\boldsymbol{h}}_{i,\mathrm{R},m}$ has all zero elements except for the m-th element, which is given by $P_{i,m,\mathrm{sig}}/P_{i,m}$. The corresponding interference power (including the ICI and the ISI) is calculated as $P_{i\mathrm{R},m,\mathrm{int}} = \boldsymbol{z}_{i,\mathrm{R},m}^{\mathrm{T}} \boldsymbol{p}_i$. The vector $\boldsymbol{z}_{i,\mathrm{R},m}$ has also all zero elements except for the $(m-1)$-th, m-th, and $(m+1)$-th elements, which are $\boldsymbol{a}_{i,m-1}^{\mathrm{T}} \boldsymbol{G}_{i,m,m-1}[k] \boldsymbol{G}_{i,m,m-1}[k]^{\mathrm{T}} \boldsymbol{a}_{i,m-1}$, $\boldsymbol{a}_{i,m}^{\mathrm{T}} \boldsymbol{G}_{i,m,m}[k](\boldsymbol{I} - \boldsymbol{e}_\ell \boldsymbol{e}_\ell^{\mathrm{T}}) \boldsymbol{G}_{i,m,m}[k]^{\mathrm{T}} \boldsymbol{a}_{i,m}$, and $\boldsymbol{a}_{i,m+1}^{\mathrm{T}} \boldsymbol{G}_{i,m,m+1}[k] \boldsymbol{G}_{i,m,m+1}[k]^{\mathrm{T}} \boldsymbol{a}_{i,m+1}$, respectively. Similarly, the received signal power and the interference power on the m-th subcarrier of the j-th UT are derived as $P_{\mathrm{R}j,m,\mathrm{sig}} = \bar{\boldsymbol{h}}_{\mathrm{R},j,m}^{\mathrm{T}} \boldsymbol{p}_{\mathrm{R}}$ and $P_{\mathrm{R}j,m,\mathrm{int}} = \boldsymbol{z}_{\mathrm{R},j,m}^{\mathrm{T}} \boldsymbol{p}_{\mathrm{R}}$, respectively. Note that $\bar{\boldsymbol{h}}_{\mathrm{R},j,m}$ and $\boldsymbol{z}_{\mathrm{R},j,m}$ can be obtained by replacing $\boldsymbol{a}_{i,m}$ in $\bar{\boldsymbol{h}}_{i,\mathrm{R},m}$ and $\boldsymbol{z}_{i,\mathrm{R},m}$ with $\boldsymbol{b}_{j,m}$, and by replacing $\boldsymbol{G}$ with $\tilde{\boldsymbol{G}}$. Moreover, the transmit power constraints at the UTs and at the relay are formulated as $\sum_{n=-\infty}^{+\infty} \mathbb{E}\{|s_i[n]|^2\} = \mathbf{1}^{\mathrm{T}} \boldsymbol{p}_i \leq P_{\mathrm{U}}$, $\forall i$, and $\sum_{n=-\infty}^{+\infty} \mathbb{E}\{|\bar{r}[n]|^2\} = \mathbf{1}^{\mathrm{T}} \boldsymbol{p}_{\mathrm{R}} \leq P_{\mathrm{R}}$, respectively.

Remark 1. *We can alternatively apply multi-tap filters only at the relay while the UTs only perform power allocation. In this way the computational burden of the filters at the UTs is completely moved to the relay. However, the filter design at a two-way relay is more challenging since the filter on each subcarrier has to guarantee the quality of service for both UTs.*

IV. OPTIMAL POWER CONTROL SCHEME

Let R_{12} and R_{21} denote the achievable rate from UT1 to UT2 and from UT2 to UT1 in a FBMC based DF TWR system, respectively. By applying the information-theoretic analysis in [9] and its extension to the OFDM system in [10], we can show that R_{12} and R_{21} are upper bounded by

$$\begin{aligned}
R_{12} &\leq \min\left\{\mu \sum_{m=1}^{M} I(d_{1,m}; \hat{r}_m | d_{2,m}), (1-\mu) \sum_{m=1}^{M} I(d_{\mathrm{R},m}; y_{2,m})\right\} \\
R_{21} &\leq \min\left\{\mu \sum_{m=1}^{M} I(d_{2,m}; \hat{r}_m | d_{1,m}), (1-\mu) \sum_{m=1}^{M} I(d_{\mathrm{R},m}; y_{1,m})\right\} \\
R_{12} + R_{21} &\leq \min\left\{\mu \sum_{m=1}^{M} I(d_{1,m}, d_{2,m}; \hat{r}_m)\right\} \qquad (4)
\end{aligned}$$

where μ denotes the portion of the MAC phase in a complete transmission and the time interval of a complete transmission is normalized to 1. The function $I(\cdot)$ calculates the per-subcarrier mutual information. In this paper the residual ICI and ISI after applying the multi-tap filters are treated as noise. According to [11], it can be shown that $I(d_{i,m}; \hat{r}_m | d_{j,m}) = \log_2\left(\frac{\boldsymbol{h}_{i,\mathrm{R},m}^{\mathrm{T}} \boldsymbol{p}_i + \sigma_{\mathrm{R}}^2/2}{\boldsymbol{z}_{i,\mathrm{R},m}^{\mathrm{T}} \boldsymbol{p}_i + \sigma_{\mathrm{R}}^2/2}\right)$, where $\boldsymbol{h}_{i,\mathrm{R},m} = \bar{\boldsymbol{h}}_{i,\mathrm{R},m} + \boldsymbol{z}_{i,\mathrm{R},m}$. Similarly, we have $I(d_{\mathrm{R},m}; y_{j,m}) = \log_2\left(\frac{\boldsymbol{h}_{\mathrm{R},j,m}^{\mathrm{T}} \boldsymbol{p}_{\mathrm{R}} + \sigma_{\mathrm{R}}^2/2}{\boldsymbol{z}_{\mathrm{R},j,m}^{\mathrm{T}} \boldsymbol{p}_{\mathrm{R}} + \sigma_{\mathrm{R}}^2/2}\right)$, where $\boldsymbol{h}_{\mathrm{R},j,m} = \bar{\boldsymbol{h}}_{\mathrm{R},j,m} + \boldsymbol{z}_{\mathrm{R},j,m}$, and $I(d_{1,m}, d_{2,m}; \hat{r}_m) = \log_2\left(\frac{\boldsymbol{h}_{1,\mathrm{R},m}^{\mathrm{T}} \boldsymbol{p}_1 + \boldsymbol{h}_{2,\mathrm{R},m}^{\mathrm{T}} \boldsymbol{p}_2 + \sigma_{\mathrm{R}}^2/2}{\boldsymbol{z}_{1,\mathrm{R},m}^{\mathrm{T}} \boldsymbol{p}_1 + \boldsymbol{z}_{2,\mathrm{R},m}^{\mathrm{T}} \boldsymbol{p}_2 + \sigma_{\mathrm{R}}^2/2}\right)$.

Let us define the exchange rate as $R_{\mathrm{x}} = \min(R_{12}, R_{21})$. According to [10], given a fixed μ the achievable rate region problem of the FBMC/OQAM modulated DF TWR system, i.e., the maximization of the exchange rate R_{x} subject to transmit power constraints and the rate constraints in (4), is equivalent to solving two subproblems. These are the maximization of the MAC rate and the BC rate. Define R_{MAC} and R_{BC} as the achievable exchange rate in the MAC phase and in the BC phase, respectively. The maximization of the MAC rate is formulated as

$$\begin{aligned}
&\max_{R_{\mathrm{MAC}}, \boldsymbol{p}_1, \boldsymbol{p}_2} \quad R_{\mathrm{MAC}} \\
&\text{s.t.} \quad R_{\mathrm{MAC}} \leq \mu \sum_{m=1}^{M} \log_2\left(\frac{\boldsymbol{h}_{i,\mathrm{R},m}^{\mathrm{T}} \boldsymbol{p}_i + \sigma_{\mathrm{R}}^2/2}{\boldsymbol{z}_{i,\mathrm{R},m}^{\mathrm{T}} \boldsymbol{p}_i + \sigma_{\mathrm{R}}^2/2}\right), \; i = 1, 2 \\
&\qquad R_{\mathrm{MAC}} \leq \frac{\mu}{2} \sum_{m=1}^{M} \log_2\left(\frac{\boldsymbol{h}_{1,\mathrm{R},m}^{\mathrm{T}} \boldsymbol{p}_1 + \boldsymbol{h}_{2,\mathrm{R},m}^{\mathrm{T}} \boldsymbol{p}_2 + \sigma_{\mathrm{R}}^2/2}{\boldsymbol{z}_{1,\mathrm{R},m}^{\mathrm{T}} \boldsymbol{p}_1 + \boldsymbol{z}_{2,\mathrm{R},m}^{\mathrm{T}} \boldsymbol{p}_2 + \sigma_{\mathrm{R}}^2/2}\right) \\
&\qquad \mathbf{1}^{\mathrm{T}} \boldsymbol{p}_1 \leq P_{\mathrm{U}}, \mathbf{1}^{\mathrm{T}} \boldsymbol{p}_2 \leq P_{\mathrm{U}}, \qquad (5)
\end{aligned}$$

and the maximization of the BC rate is given by

$$\begin{aligned}
&\max_{R_{\mathrm{BC}}, \boldsymbol{p}_{\mathrm{R}}} \quad R_{\mathrm{BC}} \\
&\text{s.t.} \quad R_{\mathrm{BC}} \leq (1-\mu) \sum_{m=1}^{M} \log_2\left(\frac{\boldsymbol{h}_{\mathrm{R},j,m}^{\mathrm{T}} \boldsymbol{p}_{\mathrm{R}} + \sigma_{\mathrm{R}}^2/2}{\boldsymbol{z}_{\mathrm{R},j,m}^{\mathrm{T}} \boldsymbol{p}_{\mathrm{R}} + \sigma_{\mathrm{R}}^2/2}\right), \; j = 1, 2 \\
&\qquad \mathbf{1}^{\mathrm{T}} \boldsymbol{p}_{\mathrm{R}} \leq P_{\mathrm{R}}. \qquad (6)
\end{aligned}$$

The optimal solution of (5) and (6) are also optimal for the original rate region problem. This is due to the fact that the power control at the UTs, which is only relevant in the MAC phase, is not coupled with the power control at the relay, which is only relevant in the BC phase. We have $R_{\mathrm{x}} = \min(R_{\mathrm{MAC}}, R_{\mathrm{BC}})$. Unlike its CP-OFDM counterpart in [10], these two subproblems are non-convex due to the residual ICI and ISI terms, i.e., the logarithmic terms in the constraints are non-convex. In the following, we devise an efficient convex optimization based iterative method to solve (5). The same method can be used to solve problem (6) since it has the same structure as (5).

The first constraint in (5) can be rewritten as

$$\begin{aligned}
&R_{\mathrm{MAC}} - \mu \sum_{m=1}^{M} \log_2\left(\boldsymbol{h}_{i,\mathrm{R},m}^{\mathrm{T}} \boldsymbol{p}_i + \sigma_{\mathrm{R}}^2/2\right) \\
&\quad + \mu \sum_{m=1}^{M} \log_2\left(\boldsymbol{z}_{i,\mathrm{R},m}^{\mathrm{T}} \boldsymbol{p}_i + \sigma_{\mathrm{R}}^2/2\right) \leq 0. \qquad (7)
\end{aligned}$$

Since the logarithmic function is a concave function [12], it can be shown that all the logarithmic terms in (7) are concave with respect to $\boldsymbol{p}_i$. Thus, the left-hand side of equation (7) contains differences of concave functions (DC), which are non-convex. The non-convexity lies in the logarithmic terms with plus signs. To mitigate the non-convexity, we introduce an auxiliary variable t_i and reformulate (7) into the following two constraints

$$\begin{aligned}
&R_{\mathrm{MAC}} - \mu \sum_{m=1}^{M} \log_2\left(\boldsymbol{h}_{i,\mathrm{R},m}^{\mathrm{T}} \boldsymbol{p}_i + \sigma_{\mathrm{R}}^2/2\right) + t_i \leq 0 \\
&\mu \sum_{m=1}^{M} \log_2\left(\boldsymbol{z}_{i,\mathrm{R},m}^{\mathrm{T}} \boldsymbol{p}_i + \sigma_{\mathrm{R}}^2/2\right) - t_i \leq 0. \qquad (8)
\end{aligned}$$

Clearly, the non-convexity is now in the second inequality. To deal with it, we propose to use a linear approximation of the logarithmic function of multivariate (vector) variables, e.g., the first order Taylor series of the logarithmic function. The first order polynomial approximation of $\log_2\left(\boldsymbol{z}_{i,\mathrm{R},m}^{\mathrm{T}}\boldsymbol{p}_i+\sigma_{\mathrm{R}}^2/2\right)$ at a vector $\boldsymbol{p}_{i,\mathrm{ini}}$ is given by

$$\log_2\left(\boldsymbol{z}_{i,\mathrm{R},m}^{\mathrm{T}}\boldsymbol{p}_i+\sigma_{\mathrm{R}}^2/2\right)\approx\frac{1}{\log(2)}\Bigg(\log\left(\boldsymbol{z}_{i,\mathrm{R},m}^{\mathrm{T}}\boldsymbol{p}_{i,\mathrm{ini}}+\sigma_{\mathrm{R}}^2/2\right)+\frac{\boldsymbol{z}_{i,\mathrm{R},m}^{\mathrm{T}}}{\boldsymbol{z}_{i,\mathrm{R},m}^{\mathrm{T}}\boldsymbol{p}_{i,\mathrm{ini}}+\sigma_{\mathrm{R}}^2/2}(\boldsymbol{p}_i-\boldsymbol{p}_{i,\mathrm{ini}})\Bigg) \tag{9}$$

Note that the same linear approximation can be applied for all m. The constraints (8) can be modified as

$$\begin{aligned}&R_{\mathrm{MAC}}-\mu\sum_{m=1}^{M}\log_2\left(\boldsymbol{h}_{i,\mathrm{R},m}^{\mathrm{T}}\boldsymbol{p}_i+\sigma_{\mathrm{R}}^2/2\right)+t_i\le 0\\ &\mu\sum_{m=1}^{M}\frac{1}{\log(2)}\Bigg(\log\left(\boldsymbol{z}_{i,\mathrm{R},m}^{\mathrm{T}}\boldsymbol{p}_{i,\mathrm{ini}}+\sigma_{\mathrm{R}}^2/2\right)\\ &+\frac{\boldsymbol{z}_{i,\mathrm{R},m}^{\mathrm{T}}}{\boldsymbol{z}_{i,\mathrm{R},m}^{\mathrm{T}}\boldsymbol{p}_{i,\mathrm{ini}}+\sigma_{\mathrm{R}}^2/2}(\boldsymbol{p}_i-\boldsymbol{p}_{i,\mathrm{ini}})\Bigg)-t_i\le 0.\end{aligned} \tag{10}$$

Clearly, for a fixed $\boldsymbol{p}_{i,\mathrm{ini}}$, all the constraints in (10) are convex. The other two non-convex constraints can be convexified in the same way. Finally, problem (5) is reformulated as

$$\begin{aligned}&\max_{R_{\mathrm{MAC}},\boldsymbol{p}_1,\boldsymbol{p}_2,t_{\mathrm{s}},t_i,\forall i}\quad R_{\mathrm{MAC}}\\ \text{s.t.}\quad &R_{\mathrm{MAC}}-\mu\sum_{m=1}^{M}\log_2\left(\boldsymbol{h}_{i,\mathrm{R},m}^{\mathrm{T}}\boldsymbol{p}_i+\sigma_{\mathrm{R}}^2/2\right)+t_i\le 0, i=1,2\\ &\mu\sum_{m=1}^{M}\frac{1}{\log(2)}\Bigg(\log\left(\boldsymbol{z}_{i,\mathrm{R},m}^{\mathrm{T}}\boldsymbol{p}_{i,\mathrm{ini}}+\sigma_{\mathrm{R}}^2/2\right)\\ &+\frac{\boldsymbol{z}_{i,\mathrm{R},m}^{\mathrm{T}}}{\boldsymbol{z}_{i,\mathrm{R},m}^{\mathrm{T}}\boldsymbol{p}_{i,\mathrm{ini}}+\sigma_{\mathrm{R}}^2/2}(\boldsymbol{p}_i-\boldsymbol{p}_{i,\mathrm{ini}})\Bigg)-t_i\le 0,\ i=1,2\\ &R_{\mathrm{MAC}}\le\frac{\mu}{2}\sum_{m=1}^{M}\log_2\left(\sum_{i=1}^{2}\boldsymbol{h}_{i,\mathrm{R},m}^{\mathrm{T}}\boldsymbol{p}_i+\sigma_{\mathrm{R}}^2/2\right)-t_{\mathrm{s}},\\ &\mu\sum_{m=1}^{M}\frac{1}{\log(2)}\Bigg(\log\left(\sum_{i=1}^{2}\boldsymbol{z}_{i,\mathrm{R},m}^{\mathrm{T}}\boldsymbol{p}_{i,\mathrm{ini}}+\sigma_{\mathrm{R}}^2/2\right)\\ &+\frac{\sum_{i=1}^{2}\boldsymbol{z}_{i,\mathrm{R},m}^{\mathrm{T}}(\boldsymbol{p}_i-\boldsymbol{p}_{i,\mathrm{ini}})}{\sum_{i=1}^{2}\boldsymbol{z}_{i,\mathrm{R},m}^{\mathrm{T}}\boldsymbol{p}_{i,\mathrm{ini}}+\sigma_{\mathrm{R}}^2/2}\Bigg)-t_{\mathrm{s}}\le 0,\\ &\mathbf{1}^{\mathrm{T}}\boldsymbol{p}_1\le P_{\mathrm{U}},\mathbf{1}^{\mathrm{T}}\boldsymbol{p}_2\le P_{\mathrm{U}},\end{aligned} \tag{11}$$

Since the objective function and the constraints are convex, problem (11) is a convex problem and thus can be solved efficiently using the interior-point algorithm in [12]. However, the best initial vectors $\boldsymbol{p}_{i,\mathrm{ini}}$, $\forall i$, are unknown. It is therefore natural to use an iterative method and update the initial vectors in each iteration. Here, the initial vectors $\boldsymbol{p}_{i,\mathrm{ini}}^{(o)}$, $\forall i$, at the o-th step are the optimal solutions of $\boldsymbol{p}_i$, which are obtained by solving problem (11) at the $(o-1)$-th step. Note that if problem (11) is solvable at the o-th step, then the corresponding optimal value $R_{\mathrm{MAC}}^{(o)}$ should be larger than or equal to the optimal value for the same problem at the $(o-1)$-th step, i.e., $R_{\mathrm{MAC}}^{(o-1)}$. Otherwise, if $R_{\mathrm{MAC}}^{(o)}<R_{\mathrm{MAC}}^{(o-1)}$, it is contradictory to the objective function. Moreover, the vectors $\boldsymbol{p}_{i,\mathrm{ini}}$ are bounded from below and above because $\boldsymbol{p}_i$ are bounded, $\forall i$. Hence, only a finite number of iterations is required. Furthermore, the solution generated by this iterative method converges to the Karush-Kuhn-Tucker (KKT) point of the original problem (5). This can be derived straightforwardly from Proposition 3.2 of [13]. Summarizing, the proposed method provides a polynomial time solution and the generated sequences converge to at least a local optimum of problem (5). Finally, the proposed joint design of pre-equalizers and the power control scheme in the MAC phase is described in Algorithm 1. The same method can be used to solve problem (6). We do not show the details due to the space limitation.

Remark 2. *The linear approximation of the log function has also been used to solve a problem with the sum of DC terms in our previous work [7]. There, it is proposed to use the first order Taylor expansion of the log function with a scalar variable, e.g.,* $\log(\alpha)$*. The same approach could be also used to convert each non-convex term and it would introduce* $6M$ *additional constraints. In contrast, the proposed iterative design uses the Taylor expansion of the log function with a vector-valued variable, and only* 3 *additional constraints are introduced. Thus, the proposed iterative design is computationally more efficient when* M *is large.*

Algorithm 1 Iterative algorithm for solving the MAC rate region problem (5)

Initialize: input: $h_{i,\mathrm{R}}[n]$, $\forall i$, set $o=0$, $\boldsymbol{p}_{i,\mathrm{ini}}=\mathbf{1}P_{\mathrm{U}}/M$, $R_{\mathrm{MAC}}^{(0)}=0$, and the threshold value ϵ.
Main step:
Find SLNR based solutions $\boldsymbol{a}_{i,m}$, $\forall i,m$ as in Section III, and compute $\boldsymbol{h}_{i,\mathrm{R},m}$ and $\boldsymbol{z}_{i,\mathrm{R},m}$, $\forall i,m$.
repeat
    $o=o+1$
    Solve problem (11) in order to find the optimal value $R_{\mathrm{MAC}}^{(o)}$ and $\boldsymbol{p}_i^{(o)}$, $i=1,2$.
    $\boldsymbol{p}_{i,\mathrm{ini}}=\boldsymbol{p}_i^{(o)}$, $\forall i$
until $\left|R_{\mathrm{MAC}}^{(o)}-R_{\mathrm{MAC}}^{(o-1)}\right|\le\epsilon$

V. SIMULATION RESULTS AND CONCLUDING REMARKS

The proposed iterative design is evaluated using Monte-Carlo simulations. The maximum transmit power at all nodes is set to unity and identical noise variances are assumed such that $\sigma_{\mathrm{U}}^2=\sigma_{\mathrm{R}}^2=\sigma_{\mathrm{n}}^2$. The SNR is defined as $\mathrm{SNR}=1/(M\sigma_{\mathrm{n}}^2)$. We consider the Vehicular A and the Vehicular B channel models as in [4]. The sampling frequency is set to 15.36 MHz and the subcarrier spacing is 15 kHz, which implies $M=1024$ subcarriers in total.

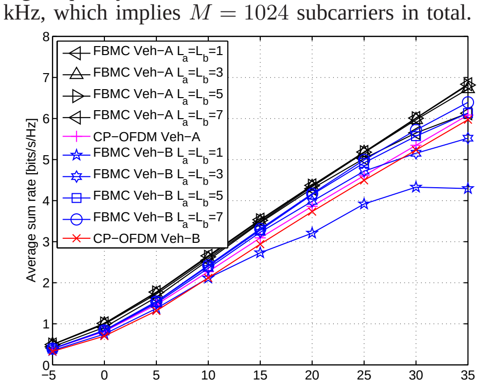

Fig. 1. Achievable sum rate vs. SNR for $\mu=0.5$, $M=1024$, $L_a=L_b$. For CP-OFDM 12.5 % CP is applied.

Fig. 1 shows that the achievable sum rate increases as the number of taps increases. A $12.5\,\%$ gain, i.e., the spectral efficiency loss due to the CP part, over CP-OFDM is achieved especially when the length of the multi-tap filters is sufficiently large. To have a trade-off between the computational complexity and the system performance, we recommend to use $L_a=L_b=5$.

ACKNOWLEDGMENTS

The authors acknowledge the financial support by the European Union FP7-ICT project EMPhAtiC (http://www.ict-emphatic.eu) under grant agreement no. 318362.

VI. REFERENCES

[1] B. Farhang-Boroujeny, "OFDM versus filter bank multicarrier," *IEEE Signal Processing Magazine*, vol. 5, 2011.

[2] M. Renfors, F. Bader, L. Baltar, D. Le Ruyet, D. Roviras, P. Mege, and M. Haardt, "On the use of filter bank based multicarrier modulation for professional mobile radio," in *Proc. 77th IEEE Vehicular Technology Conf. (VTC 2013 Spring)*, Dresden, Germany, June 2013.

[3] T. Ihalainen, T. H. Stitz, M. Rinne, and M. Renfors, "Channel equalization in filter bank based multicarrier modulation for wireless communications," *EURASIP Journal Applied Signal Processing*, Jan. 2007.

[4] M. Caus and A. I. Perez-Neira, "Transmitter-receiver design for highly frequency selective channels in MIMO FBMC systems," *IEEE Transactions on Signal Processing*, vol. 60, Dec. 2012.

[5] M. Shaat and F. Bader, "Comparison of OFDM and FBMC performance in multi-relay cognitive radio network," in *Proc. Int. Symp. Wireless Communication Systems (ISWCS)*, Paris, France, Aug. 2012.

[6] A. Alsharoa, F. Bader, and M. Alouini, "Relay selection and resource allocation for two-way DF-AF cognitive radio networks," *IEEE Wireless Communications Letters*, vol. 2, Aug. 2013.

[7] J. Zhang, S. A. Vorobyov, A. Khabbazibasmenj, and M. Haardt, "Sum rate maximization in multi-operator two-way relay networks with a MIMO AF relay via POTDC," in *Proc. 21st European Signal Processing Conference (EUSIPCO 2013)*, Marrakech, Morocco, Sept. 2013.

[8] P. Siohan, C. Siclet, and N. Lacaille, "Analysis and design of ofdm/oqam systems based on filterbank theory," *IEEE Transactions on Signal Processing*, May 2002.

[9] T. J. Oechtering, E. A. Jorswieck, R. F. Wyrembelski, and H. Boche, "On the optimal transmit strategy for the MIMO bidirectional broadcast channel," *IEEE Transactions on Communications*, Dec. 2009.

[10] F. He, X. Chen, L. Xiao, and S. Zhou, "Optimal power allocation for two-way decode-and-forward OFDM relay networks," in *Proc. IEEE International Conference on Communications (ICC 2012)*, Ottawa, Canada, June 2012.

[11] T. M. Cover and J. A. Thomas, *Elements of information theory*, John Wiley and Sons, Inc., 2006.

[12] S. Boyd and L. Vandenberghe, *Convex Optimization*, Cambridge, U.K., 2004.

[13] A. Beck, A. B.-Tal, and L. Tetruashvili, "A sequential parametric convex approximation method with applications to nonconvex truss topology design problems," *J. Global Optim.*, vol. 47, no. 1, 2010.